

# Anisotropy of the quark-antiquark potential in a magnetic field

Claudio Bonati,<sup>\*</sup> Massimo D'Elia,<sup>†</sup> Marco Mariti,<sup>‡</sup> Michele Mesiti,<sup>§</sup> and Francesco Negro<sup>¶</sup>  
*Dipartimento di Fisica dell'Università di Pisa and INFN - Sezione di Pisa,*  
*Largo Pontecorvo 3, I-56127 Pisa, Italy*

Francesco Sanfilippo<sup>\*\*</sup>

*School of Physics and Astronomy, University of Southampton, SO17 1BJ Southampton, United Kingdom*

(Dated: June 15, 2018)

We investigate the static  $\bar{Q}Q$ -potential for  $N_f = 2+1$  QCD at the physical point in the presence of a constant and uniform external magnetic field. The potential is found to be anisotropic and steeper in the directions transverse to the magnetic field than in the longitudinal one. In particular, when compared to the standard case with zero background field, the string tension increases (decreases) in the transverse (longitudinal) direction, while the absolute value of the Coulomb coupling and the Sommer parameter show an opposite behavior.

PACS numbers: 12.38.Aw, 11.15.Ha, 12.38.Gc, 12.38.Mh

## I. INTRODUCTION

The properties of strong interactions in the presence of a strong magnetic background have attracted much interest in the last few years (see, e.g., Ref. [1] for recent reviews). This is justified by the many contexts in which such properties may play a role: the physics of compact astrophysical objects [2], of non-central heavy ion collisions [3–7] and of the early Universe [8, 9], involves fields going from  $10^{10}$  Tesla up to  $10^{16}$  Tesla ( $|e|B \sim 1 \text{ GeV}^2$ ).

One important feature is that gluon fields, even if not directly coupled to electromagnetic fields, may undergo significant modifications, through effective QED-QCD interactions induced by quark loop effects [10–24]. Such a possibility has been confirmed by lattice QCD simulations [25–32], resulting also in unexpected behaviors, like inverse magnetic catalysis [27, 31–41].

One of the main attributes of strong interactions is the appearance of a confining potential. In the heavy quark limit, that is related to the expectation value of Wilson loops, so that the potential emerges as a property of gauge fields only. It is interesting, then, to ask whether a magnetic background can influence the static quark-antiquark potential. Many studies have considered the possible emergence of anisotropies [10, 11, 16, 22], which may have many phenomenological implications, like a modification of the heavy quark bound states.

On the lattice, anisotropies in the gauge field distributions have already been observed in quantities like the average plaquettes taken in different planes [28, 29]. However, an investigation of the possible anisotropies of the static potential is still missing.

In this paper, we present an exploratory study of this issue, based on numerical simulations of  $N_f = 2 + 1$  QCD with physical quark masses, discretized by stout improved staggered fermions and the tree level improved Symanzik gauge action. In particular, we look at the expectation values of Wilson loops in the presence of a magnetic background, and compute from them the static potential for quark-antiquark separations orthogonal or parallel to the magnetic field. We consider zero temperature, three different lattice spacings and magnetic fields up to  $|e|B \sim 1 \text{ GeV}^2$ . Results show the emergence of anisotropies both in the string tension and in the Coulomb part of the potential.

## II. NUMERICAL METHODS

We have considered a constant and uniform magnetic field, which enters the QCD Lagrangian through quark covariant derivatives  $D_\mu = \partial_\mu + igA_\mu^a T^a + iq_f A_\mu$ , where  $A_\mu$  is the Abelian gauge potential and  $q_f$  is the quark electric charge. On the lattice, that amounts to adding proper  $U(1)$  phases to the usual  $SU(3)$  links entering the Dirac operator. The Euclidean partition function is expressed as

$$\mathcal{Z}(B) = \int \mathcal{D}U e^{-\mathcal{S}_{YM}} \prod_{f=u,d,s} \det(D_{\text{st}}^f[B])^{1/4}, \quad (1)$$

$$\mathcal{S}_{YM} = -\frac{\beta}{3} \sum_{i,\mu \neq \nu} \left( \frac{5}{6} W_{i;\mu\nu}^{1 \times 1} - \frac{1}{12} W_{i;\mu\nu}^{1 \times 2} \right), \quad (2)$$

$$(D_{\text{st}}^f)_{i,j} = am_f \delta_{i,j} + \sum_{\nu=1}^4 \frac{\eta_{i;\nu}}{2} \left( u_{i;\nu}^f U_{i;\nu}^{(2)} \delta_{i,j-\hat{\nu}} - u_{i-\hat{\nu};\nu}^{f*} U_{i-\hat{\nu};\nu}^{(2)\dagger} \delta_{i,j+\hat{\nu}} \right) \quad (3)$$

where  $\mathcal{D}U$  is the functional integration over the  $SU(3)$  link variables.  $\mathcal{S}_{YM}$  is the tree level improved Symanzik action [44, 45], involving the real part of the trace of

<sup>\*</sup>Electronic address: bonati@df.unipi.it

<sup>†</sup>Electronic address: delia@df.unipi.it

<sup>‡</sup>Electronic address: mariti@df.unipi.it

<sup>§</sup>Electronic address: mesiti@df.unipi.it

<sup>¶</sup>Electronic address: fnegro@pi.infn.it

<sup>\*\*</sup>Electronic address: f.sanfilippo@soton.ac.uk

the  $1 \times 1$  ( $W_{i;\mu\nu}^{1 \times 1}$ ) and  $1 \times 2$  ( $W_{i;\mu\nu}^{1 \times 2}$ ) loops.  $D_{\text{st}}^f$  is the staggered Dirac operator, built up by two times stout-smearing links  $U_{i;\mu}^{(2)}$  [46] (with isotropic smearing parameters  $\rho_{\mu\nu} = 0.15 \delta_{\mu\nu}$ ), in order to reduce finite cut-off effects, in particular taste symmetry violations (see [47] for a comparison of the effectiveness in reducing taste violations of the different improved staggered discretizations).

The Abelian continuum gauge field  $A_y = Bx$  and  $A_\mu = 0$  for  $\mu = t, x, z$ , corresponding to a magnetic field in the  $\hat{z}$  direction, is discretized on the lattice torus as

$$u_{i;y}^f = e^{ia^2 q_f B i_x}, \quad u_{i;x}^f|_{i_x=L_x} = e^{-ia^2 q_f L_x B i_y} \quad (4)$$

with  $u_{i;\mu}^f = 1$  elsewhere and  $B$  is quantized as [48–51]

$$|e|B = 6\pi b / (a^2 L_x L_y); \quad b \in \mathbb{Z}. \quad (5)$$

No stout smearing is applied to the  $U(1)$  phases, which are treated as purely external parameters (quenched QED approximation).

We performed simulations at the physical value of the pion mass,  $m_\pi \sim 135$  MeV, and three different values of the lattice spacing  $a$ , using the bare parameters reported in Table I ( $m_s/m_{u,d}$  is fixed to its physical value, 28.15). In Ref. [42] it was shown that making use of different standard observables (like for instance  $m_K$  or  $f_K$ ) to determine the physical point, compatible results are obtained, so we do not expect large cut-off effects to be present. We explored symmetric, zero temperature lattices, with the number of sites per direction ( $L$ ) tuned to maintain  $La \simeq 5$  fm. The Rational Hybrid Monte-Carlo (RHMC) algorithm was used to sample gauge configurations, with statistics ranging, for each value of  $B$ , from  $O(10^4)$  to  $O(10^3)$  molecular dynamics (MD) time units, going from the coarsest to the finest lattice.

In order to determine the spin-averaged potential between a static  $\bar{Q}Q$  pair, separated by a distance  $\vec{R}$ , we considered the large time behavior of the average rectangular Wilson loop  $W(\vec{R}, T)$ , where  $T$  is the time extension of the loop. Usually, based on space-time isotropy, one averages over all directions of  $\vec{R}$ ; on the contrary, apart from the  $B = 0$  case, we considered separately the averages over different directions, thus leaving room to the possibility that  $V(\vec{R})$  may not be a central potential.

Going to a lattice notation, in which  $\vec{n}$  and  $n_t$  denote the dimensionless spatial and temporal sides of the loop,

$L$	$a(\text{fm})$	$\beta$	$am_{u/d}$	$am_s$	$b$
24	0.2173(4)	3.55	0.003636	0.1020	0,12,16,24,32,40
32	0.1535(3)	3.67	0.002270	0.0639	0,12,16,24,32,40
40	0.1249(3)	3.75	0.001787	0.0503	0,8,12,16,24,32,40

TABLE I: Simulation parameters, chosen according to Refs. [42, 43] and corresponding to a physical pion mass. The systematic error on  $a$  is about 2% [42].

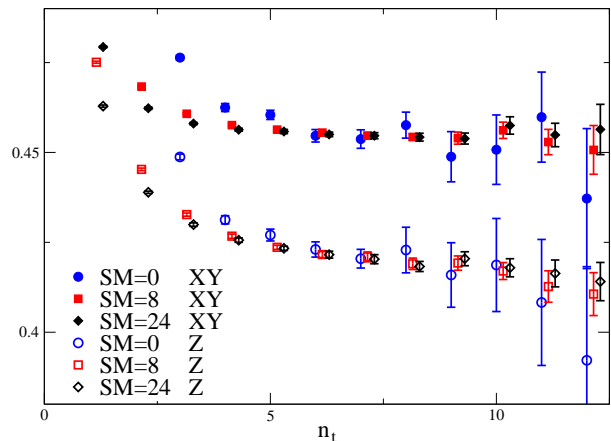


FIG. 1: Wilson loop combination defined in Eq. (6) for  $|\vec{n}| = 3$  as a function of  $n_t$  and for several values of the APE smearing level. The simulation was performed on the  $32^4$  lattice at  $|e|B = 0.97$  GeV<sup>2</sup>.

the potential can be obtained as

$$aV(a\vec{n}) = \lim_{n_t \rightarrow \infty} \log \left( \frac{\langle W(a\vec{n}, a n_t) \rangle}{\langle W(a\vec{n}, a(n_t + 1)) \rangle} \right). \quad (6)$$

In practice, one plots the right-hand side as a function of  $n_t$  and looks for a stable plateau at large times, from which the potential can be extracted by a fit to a constant function. In the present study we limit ourselves to the cases of  $\vec{n}$  parallel or orthogonal to  $\vec{B}$ .

For each simulation, we measured Wilson loops every 5 MD time units. In order to reduce the UV noise, we applied one step of HYP smearing [52] for temporal links, with smearing parameters corresponding to the so-called HYP2-action of Ref. [53], and  $N_{SM}$  steps of APE-smearing [54] for spatial links, with smearing parameter  $\alpha_{APE} = 0.25$ .

Since APE-smearing treats all spatial directions symmetrically, it is important to check that possible anisotropies be not washed out by this noise reduction technique. We studied, for a few cases, the dependence of results on the number of smearing steps and, having checked that it is not significant (see next section), we fixed  $N_{SM} = 24$ . The statistical errors on the right-hand side of Eq. (6), as well as those on the parameters of the fitted plateaux, were determined by performing a bootstrap analysis to take correlations into account.

### III. NUMERICAL RESULTS

In Fig. 1 we report an example of the logarithm of Wilson loop ratios, see Eq. (6), as a function of  $n_t$  and for different APE-smearing levels, obtained at spatial distance  $|\vec{n}| = 3$  and for  $|e|B = 0.97$  GeV<sup>2</sup>. We show separately results averaged over the longitudinal ( $Z$ ) or transverse ( $XY$ ) directions. A well defined plateau is visible in both cases, and the emergence of anisotropies clearly appears,

with the potential being larger in the transverse direction. It is also evident that smearing has no visible effect on such anisotropies, so that one can safely adopt a number of smearing levels large enough to have a good noise/signal ratio.

In Fig. 2 we report an example of the potential, as a function of the  $\bar{Q}Q$  separation, determined for our smallest lattice spacing and for two values of the magnetic field,  $eB = 0$  and  $eB \simeq 0.7 \text{ GeV}^2$  ( $b = 24$ ). In the former case we averaged over all spatial directions. For  $B \neq 0$  we observe a clear anisotropic behavior, with a striking separation of the values of the potential measured along the  $Z$  or  $XY$  directions. A comparison with  $B = 0$  shows that the potential increases in the transverse directions and decreases in the longitudinal direction. This behavior is observed for all the explored lattice spacings, starting from magnetic fields of the order  $eB \simeq 0.2 \text{ GeV}^2$ .

In the same figure we also show, for  $B \neq 0$ , the potential obtained by averaging Wilson loops over all spatial directions (denoted by  $XYZ$ ). It is interesting to notice that in this case the effect of  $B$  on the static potential is strongly reduced. This fact may explain why previous studies have not observed significant effects of the external field on the static potential [27].

In order to characterize the dependence of the potential on the magnetic field, we fitted it, for each value of  $B$  and for transverse and longitudinal directions separately, according to the standard Cornell parametrization:

$$aV(an\hat{d}) = \hat{c}_d + \hat{\sigma}_d n + \frac{\alpha_d}{n}, \quad (7)$$

where  $\hat{d}$  is a versor along the  $z$  or  $xy$  directions,  $\hat{\sigma}_d$  is the string tension,  $\alpha_d$  the Coulomb coupling, and  $\hat{c}_d$  a constant term (the index  $d$  takes into account the possible dependence on the direction). Such a parametrization fits reasonably well the measured potentials, with  $\chi^2/\text{d.o.f.} \lesssim 1$  for all the explored fields and in a distance range going from  $\sim 0.3$  to  $\sim 1$  fm. In our fits we set  $\alpha_d = \hat{r}_{0d}^2 \hat{\sigma}_d - 1.65$ , in order to determine the string tension and the Sommer parameter  $\hat{r}_{0d}$  as independent quantities. A bootstrap analysis has been performed to determine the statistical errors of the fit parameters.

In order to monitor the dependence of the fitted parameters on  $B$ , we normalize them to the values they take for  $B = 0$  at the same lattice spacing, i.e. we determine the quantities

$$R^{\mathcal{O}_d} = \frac{\mathcal{O}_d(|e|B)}{\mathcal{O}_d(|e|B=0)}, \quad (8)$$

which are shown in Figs. 3, 4 and 5, respectively for  $\mathcal{O}_d = \hat{r}_{0d}$ ,  $\hat{\sigma}_d$ , and  $\alpha_d$ .

The observed anisotropy in the potential reflects in these quantities, leading to a significant splitting of the corresponding ratios, which are of the order of 10 – 20%. In particular, the string tension increases (decreases), as a function of  $eB$ , in the transverse (longitudinal) direction, while the  $\hat{r}_0$  and the Coulomb coupling show an opposite behavior.

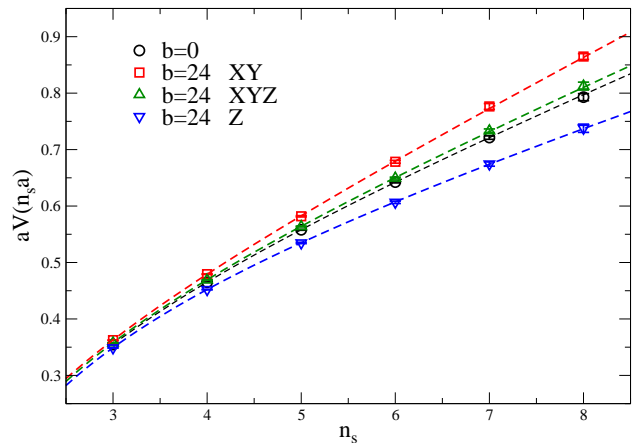


FIG. 2:  $\bar{Q}Q$ -potential both for  $|e|B = 0$  and for  $|e|B = 0.7 \text{ GeV}^2$  on the  $40^4$  lattice.

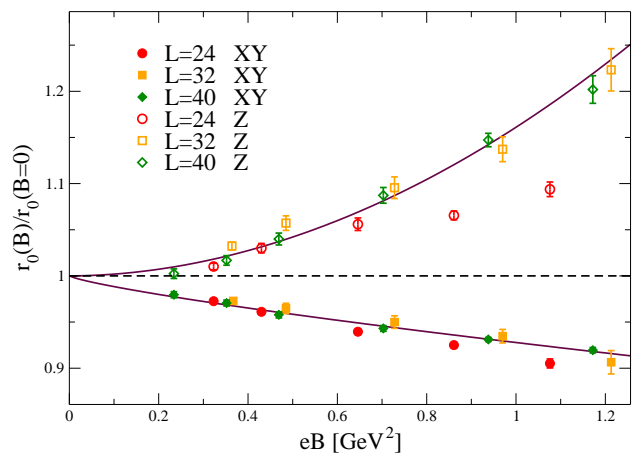


FIG. 3:  $R^{r_0}$  along the  $Z$  and  $XY$  directions. The solid line is the fit according to Eq. (9) for the  $L = 40$  data: we obtained  $A^{r_{0xy}} = -0.072(2)$ ,  $C^{r_{0xy}} = 0.79(5)$  with  $\chi^2/\text{d.o.f.} = 0.59$  and  $A^{r_{0z}} = 0.161(6)$ ,  $C^{r_{0z}} = 1.9(1)$  with  $\chi^2/\text{d.o.f.} = 1.28$ .

Our results show a mild dependence on the lattice spacing, apart from the largest fields on the coarsest lattice, for which  $eB \sim 1/a^2$ ; however the present accuracy of our data does not permit a proper continuum extrapolation. We fit the  $L = 40$  data (corresponding to our finest lattice spacing) according to the following ansatz for the dependence of each ratio on  $B$ :

$$R^{\mathcal{O}_d} = 1 + A^{\mathcal{O}_d} (|e|B)^{C^{\mathcal{O}_d}}; \quad (9)$$

the best fit results are shown as solid lines in the figures.

#### IV. DISCUSSION AND CONCLUSIONS

The weak dependence of our data on  $a$  suggests that what we observed is a genuine continuum phenomenon. However, it is important to exclude other possibilities, like for instance a non-trivial, anisotropic dependence of

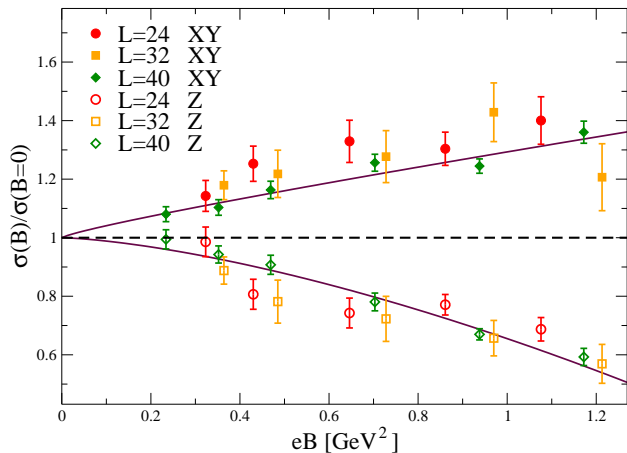


FIG. 4:  $R^\sigma$  along the  $Z$  and  $XY$  directions. The solid line is the fit according to Eq. (9) for the  $L = 40$  data: we obtained  $A^{\sigma_{xy}} = 0.29(2)$ ,  $C^{\sigma_{xy}} = 0.9(1)$  with  $\chi^2/\text{d.o.f.} = 1.14$  and  $A^{\sigma_z} = -0.34(1)$ ,  $C^{\sigma_z} = 1.5(1)$  with  $\chi^2/\text{d.o.f.} = 0.92$ .

the lattice spacing on  $B$ . In particular, an increase of  $a_z$  and a decrease of  $a_{xy}$  as a function of  $B$  would lead to similar observations. Indeed, the magnetic field in the  $\hat{z}$  direction breaks the original  $SO(4)$  symmetry of the Euclidean theory down to a  $SO(2)_{xy} \times SO(2)_{zt}$  symmetry. A possible effect, in the lattice regularized theory, could be an anisotropy in the lattice spacings, which however should still respect  $a_z = a_t$  and  $a_x = a_y$ .

An investigation of the dependence of the lattice spacing on  $B$  has been reported in Ref. [27], leading to the conclusion that the dependence is not significant. Part of the evidence, which is based on the analysis of  $r_0$ , is not useful, in view of the fact that we observe an anisotropy for this parameter. However, the dependence of the charged pion mass on  $eB$ , which is reported in Fig. 1-left of Ref. [27] and involves both  $a_t$  (to get the physical value of the pion mass) and  $a_{xy}$  (to get the physical value of  $eB$ ) clearly shows that such a non-trivial dependence is not present, at least for  $eB$  up to  $\sim 0.4 \text{ GeV}^2$ . On the other hand the anisotropies that we observe are already clearly visible for such field values.

The physical origin of the observed anisotropy has to be searched in the effective couplings between electromagnetic and chromoelectric/chromomagnetic fields, which stem from quark loop contributions. At the perturbative level [29] the effective action predicts an increase of the chromoelectric field components orthogonal to  $\vec{B}$  (see also Ref. [16]), and a suppression of the longitudinal one; this is also in agreement with the observed anisotropies at the plaquette level [28, 29]. Since confinement is related to the formation of a chromoelectric flux-tube, this result suggests an increase (decrease) of the string tension in the direction transverse (parallel) to  $\vec{B}$ , as we have found. Possible anisotropies in the static potential have been predicted also in Ref. [10], in particular a decrease of the Coulomb coupling in the transverse direction, which is consistent with our observations.

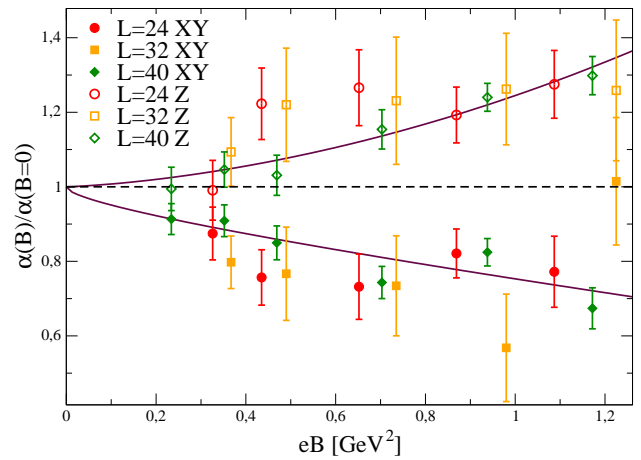


FIG. 5:  $R^\alpha$  along the  $Z$  and  $XY$  directions. The solid line is the fit according to Eq. (9) for the  $L = 40$  data: we obtained  $A^{\alpha_{xy}} = -0.24(3)$ ,  $C^{\alpha_{xy}} = 0.7(2)$  with  $\chi^2/\text{d.o.f.} = 1.53$  and  $A^{\alpha_z} = 0.24(3)$ ,  $C^{\alpha_z} = 1.7(4)$  with  $\chi^2/\text{d.o.f.} = 0.32$ .

Our exploratory study claims for extensions in various directions. While in this context we have limited ourselves to the computation of the potential in the  $Z$  and  $XY$  directions, future studies will have to investigate its dependence on the angle  $\varphi$  with respect to the magnetic field direction. On general grounds, this dependence is expected to be even in  $\cos \varphi$  (by charge conjugation invariance). Another interesting feature of the modifications in the potential, which should be better understood in the future, is the fact that they get largely suppressed when one averages Wilson loops over all spatial directions. A study of the flux tube profile for the various directions will be necessary to get a clear picture about  $B$ -dependent modifications of the chromoelectric fields. The possibility that the string tension may vanish in the  $z$  direction, for some critical value  $B$ , is another interesting issue for further investigation.

Another direction is related to the possible phenomenological consequences of our findings. To that aim, it will be necessary to extend the investigation to finite temperature, in order to have predictions valid also in the context of non-central heavy ion collisions. The spectrum of mesons in the presence of a strong magnetic background has attracted much interest in the recent past [55–63], and will likely get corrections by the presence of anisotropies in the quark-antiquark potential. We stress that even slight changes in the energy levels may induce sizable corrections to cross section, production and decay rates [60, 63]. In this respect, a direct lattice measurement of heavy quark bound states in the presence of a magnetic background will also be of great importance.

Finally, the fact that inter-quark forces are different in the directions parallel or orthogonal to the magnetic field, may lead to anisotropies in the string breaking, as well as in hadronization and thermalization processes. That could have direct consequences on various experimental probes, including the elliptic flow.

## Acknowledgments

We thank M. Chernodub and E. Laermann for useful discussions. FS thanks M. Kruse for useful discussions regarding code optimization on the Blue Gene/Q machine. FN acknowledges financial support from the EU under

project Hadron Physics 3 (Grant Agreement n. 283286). This work was partially supported by the INFN SUMA project. Numerical simulations have been performed on the Blue Gene/Q Fermi machine at CINECA, based on the agreement between INFN and CINECA (under INFN projects PI12 and NPQCD).

- 
- [1] D. Kharzeev, K. Landsteiner, A. Schmitt and H. -U. Yee, Lect. Notes Phys. **871**, 1 (2013).
- [2] R. C. Duncan and C. Thompson, Astrophys. J. **392**, L9 (1992).
- [3] V. Skokov, A. Y. Illarionov and V. Toneev, Int. J. Mod. Phys. A **24**, 5925 (2009) [arXiv:0907.1396 [nucl-th]].
- [4] V. Voronyuk, V. D. Toneev, W. Cassing, E. L. Bratkovskaya, V. P. Konchakovski and S. A. Voloshin, Phys. Rev. C **83**, 054911 (2011) [arXiv:1103.4239 [nucl-th]].
- [5] A. Bzdak and V. Skokov, Phys. Lett. B **710**, 171 (2012) [arXiv:1111.1949 [hep-ph]].
- [6] W. -T. Deng and X. -G. Huang, Phys. Rev. C **85**, 044907 (2012) [arXiv:1201.5108 [nucl-th]].
- [7] K. Tuchin, Adv. High Energy Phys. **2013**, 490495 (2013) [arXiv:1301.0099].
- [8] T. Vachaspati, Phys. Lett. B **265**, 258 (1991).
- [9] D. Grasso and H. R. Rubinstein, Phys. Rept. **348**, 163 (2001) [astro-ph/0009061].
- [10] V. A. Miransky and I. A. Shovkovy, Phys. Rev. D **66**, 045006 (2002);
- [11] M. N. Chernodub, arXiv:1001.0570 [hep-ph].
- [12] M. M. Musakhanov and F. C. Khanna, hep-ph/9605232.
- [13] H. T. Elze and J. Rafelski, In \*Sandansky 1998, Frontier tests of QED and physics of the vacuum\* 425-439 [hep-ph/9806389].
- [14] H. T. Elze, B. Muller and J. Rafelski, hep-ph/9811372.
- [15] M. Asakawa, A. Majumder and B. Muller, Phys. Rev. C **81**, 064912 (2010). [arXiv:1003.2436 [hep-ph]].
- [16] B. V. Galilo and S. N. Nedelko, Phys. Rev. D **84**, 094017 (2011). [arXiv:1107.4737 [hep-ph]].
- [17] M. A. Andreichikov, V. D. Orlovsky and Y. .A. Simonov, Phys. Rev. Lett. **110**, no. 16, 162002 (2013) [arXiv:1211.6568 [hep-ph]].
- [18] T. Kojo and N. Su, Phys. Lett. B **720**, 192 (2013) [arXiv:1211.7318 [hep-ph]].
- [19] T. Kojo and N. Su, Phys. Lett. B **726**, 839 (2013) [arXiv:1305.4510 [hep-ph]].
- [20] P. Watson and H. Reinhardt, Phys. Rev. D **89**, 045008 (2014) [arXiv:1310.6050 [hep-ph]].
- [21] J. O. Andersen, W. R. Naylor and A. Tranberg, arXiv:1311.2093 [hep-ph].
- [22] S. Ozaki, Phys. Rev. D **89**, 054022 (2014) [arXiv:1311.3137 [hep-ph]].
- [23] K. Kamikado and T. Kanazawa, JHEP **1403**, 009 (2014) [arXiv:1312.3124 [hep-ph]].
- [24] N. Mueller, J. A. Bonnet and C. S. Fischer, arXiv:1401.1647 [hep-ph].
- [25] M. D'Elia, S. Mukherjee and F. Sanfilippo, Phys. Rev. D **82**, 051501 (2010) [arXiv:1005.5365 [hep-lat]].
- [26] M. D'Elia and F. Negro, Phys. Rev. D **83**, 114028 (2011) [arXiv:1103.2080 [hep-lat]].
- [27] G. S. Bali, F. Bruckmann, G. Endrodi, Z. Fodor, S. D. Katz, S. Krieg, A. Schafer and K. K. Szabo, JHEP **1202**, 044 (2012) [arXiv:1111.4956 [hep-lat]].
- [28] E. -M. Ilgenfritz, M. Kalinowski, M. Muller-Preussker, B. Petersson and A. Schreiber, Phys. Rev. D **85**, 114504 (2012) [arXiv:1203.3360 [hep-lat]].
- [29] G. S. Bali, F. Bruckmann, G. Endrodi, F. Gruber and A. Schaefer, JHEP **1304**, 130 (2013) [arXiv:1303.1328 [hep-lat]].
- [30] M. D'Elia, M. Mariti and F. Negro, Phys. Rev. Lett. **110**, 082002 (2013) [arXiv:1209.0722 [hep-lat]].
- [31] F. Bruckmann, G. Endrodi and T. G. Kovacs, JHEP **1304**, 112 (2013) [arXiv:1303.3972 [hep-lat]].
- [32] E. -M. Ilgenfritz, M. Muller-Preussker, B. Petersson and A. Schreiber, arXiv:1310.7876 [hep-lat].
- [33] I. A. Shovkovy, Lect. Notes Phys. **871**, 13 (2013) [arXiv:1207.5081 [hep-ph]].
- [34] K. Fukushima and Y. Hidaka, Phys. Rev. Lett. **110**, 031601 (2013) [arXiv:1209.1319 [hep-ph]].
- [35] V. G. Bornyakov, P. V. Buividovich, N. Cundy, O. A. Kochetkov and A. Schfer, arXiv:1312.5628 [hep-lat].
- [36] J. Chao, P. Chu and M. Huang, Phys. Rev. D **88**, 054009 (2013) [arXiv:1305.1100 [hep-ph]].
- [37] E. S. Fraga, B. W. Mintz and J. Schaffner-Bielich, Phys. Lett. B **731**, 154 (2014) [arXiv:1311.3964 [hep-ph]].
- [38] L. Yu, H. Liu and M. Huang, arXiv:1404.6969 [hep-ph].
- [39] M. Ferreira, P. Costa, O. Loureno, T. Frederico and C. Providencia, arXiv:1404.5577 [hep-ph].
- [40] R. L. S. Farias, K. P. Gomes, G. I. Krein and M. B. Pinto, arXiv:1404.3931 [hep-ph].
- [41] M. Ruggieri, L. Oliva, P. Castorina, R. Gatto and V. Greco, arXiv:1402.0737 [hep-ph].
- [42] Y. Aoki, S. Borsanyi, S. Durr, Z. Fodor, S. D. Katz, S. Krieg and K. K. Szabo, JHEP **0906**, 088 (2009) [arXiv:0903.4155 [hep-lat]].
- [43] S. Borsanyi, G. Endrodi, Z. Fodor, A. Jakovac, S. D. Katz, S. Krieg, C. Ratti and K. K. Szabo, JHEP **1011**, 077 (2010) [arXiv:1007.2580 [hep-lat]].
- [44] P. Weisz, Nucl. Phys. B **212**, 1 (1983).
- [45] G. Curci, P. Menotti and G. Paffuti, Phys. Lett. B **130**, 205 (1983) [Erratum-ibid. B **135**, 516 (1984)].
- [46] C. Morningstar and M. J. Peardon, Phys. Rev. D **69**, 054501 (2004) [hep-lat/0311018].
- [47] A. Bazavov *et al.* [HotQCD Collaboration], PoS LATTICE **2010**, 169 (2010) [arXiv:1012.1257 [hep-lat]].
- [48] G. 't Hooft, Nucl. Phys. B **153**, 141 (1979).
- [49] P. H. Damgaard and U. M. Heller, Nucl. Phys. B **309**, 625 (1988).
- [50] M. H. Al-Hashimi and U. J. Wiese, Ann. Phys. **324**, 343 (2009) [arXiv:0807.0630 [quant-ph]].
- [51] M. D'Elia, Lect. Notes Phys. **871**, 181 (2013) [arXiv:1209.0374 [hep-lat]].
- [52] A. Hasenfratz and F. Knechtli, Phys. Rev. D **64**, 034504 (2001) [hep-lat/0103029].

- [53] M. Della Morte, A. Shindler and R. Sommer, *JHEP* **0508**, 051 (2005) [hep-lat/0506008].
- [54] M. Albanese *et al.* [APE Collaboration], *Phys. Lett. B* **192** (1987) 163.
- [55] M. N. Chernodub, *Phys. Rev. Lett.* **106**, 142003 (2011) [arXiv:1101.0117 [hep-ph]].
- [56] Y. Hidaka and A. Yamamoto, *Phys. Rev. D* **87**, 094502 (2013) [arXiv:1209.0007 [hep-ph]].
- [57] M. Frasca, *JHEP* **1311**, 099 (2013) [arXiv:1309.3966 [hep-ph]].
- [58] N. Callebaut, D. Dudal and H. Verschelde, *JHEP* **1303**, 033 (2013) [arXiv:1105.2217 [hep-th]].
- [59] M. A. Andreichikov, B. O. Kerbikov, V. D. Orlovsky and Y. A. Simonov, *Phys. Rev. D* **87**, 094029 (2013) [arXiv:1304.2533 [hep-ph]].
- [60] C. S. Machado, F. S. Navarra, E. G. de Oliveira, J. Noronha and M. Strickland, *Phys. Rev. D* **88**, 034009 (2013) [arXiv:1305.3308 [hep-ph]].
- [61] C. S. Machado, S. I. Finazzo, R. D. Matheus and J. Noronha, arXiv:1307.1797.
- [62] J. Alford and M. Strickland, *Phys. Rev. D* **88**, 105017 (2013) [arXiv:1309.3003 [hep-ph]].
- [63] P. Filip, *PoS CPOD* **2013**, 035 (2013).